A&A 367, 371–380 (2001)
DOI: 10.1051/0004-6361:20000342

Astronomy & Astrophysics

Dark-speckle coronagraphic detection of binary stars in the near-IR⋆

A. Boccaletti[1], C. Moutou[2], D. Mouillet[3], A.-M. Lagrange[3], and J.-C. Augereau[3]

[1] GPS - CalTech Pasadena, CA, USA
e-mail: boccalet@gps.caltech.edu
[2] ESO Santiago, Chile
e-mail: cmoutou@eso.org
[3] LAOG, Laboratoire d'Astrophysique de Grenoble, France
e-mail: mouillet@obs.ujf-grenoble.fr; lagrange@obs.ujf-grenoble.fr; augereau@obs.ujf-grenoble.fr

Received 13 June 2000 / Accepted 28 November 2000

Abstract. In this paper, we present the first attempt to obtain images of binary stars in the near IR using the dark-speckle method on the 3.6 m telescope at La Silla. Promising results are presented, despite the effect of the detector high read-out noise affecting the efficiency of speckle observations. We give some comparisons with the long exposure method. We derive in these data a reliable limit of detection for binary star companions, around $m_K < 4$ stars, which is about $\Delta m_K \approx 6-7$ for angular separations ranging from $0.5''$ to $0.9''$.

Key words. methods: data analysis – techniques: interferometric – instrumentation: adaptives optics – binaries: close – planetary systems

1. Introduction

Dark-speckle imaging is a technique proposed in 1995 by Labeyrie to improve the detection of faint companions orbiting around bright stars. The dark-speckle method used with refined coronagraphs (Abe et al. 2000; Rouan et al. 2000; Roddier & Roddier 1997; Gay & Rabbia 1996) and densely actuated adaptive optics (Trauger 1998) is expected to provide images of exo-planetary systems. Basically, a short exposure obtained under atmospheric condition and after seeing compensation by an adaptive optics system, is composed with a bright high-resolution peak (the brightness depending on the Strehl ratio) surrounding by a halo of speckles. A coronagraph is then usually required to block out the light from the on-axis star. Nevertheless, a significant part of the starlight is scattered into a halo of speckles thus preventing the detection of very faint companions. The dark-speckle method deals with this residual halo and contributes as an additional stage of cleaning. The speckle pattern, appearing on a short exposure, originates from random interferences provided by the atmospheric seeing. The so-called "dark speckles" are regions of the focal plane where the interferences are highly destructives. Assuming a uniformly random speckle halo, zero photo-events associated with dark speckles are recorded in the field with the same probability. The principle of the dark-speckle method is based on the fact that the presence of a planet disturb the speckle statistics and can be detected by mapping successively the occurrence of the dark-speckles on each short exposure. Indeed, the 0 photo-events count will be lower at the planet location than elsewhere in the field. Actually, the statistics of the 0 photo-events is more affected than other photo-events but a huge number of short exposures are required to increase the signal to noise ratio. In this way, the dark-speckle analysis is expected to be more efficient than a classical integration regarding the detection of very faint companions (see Labeyrie 1995; Boccaletti et al. 1998a for more details).

A "Dark-Speckle Coronagraph" has been recently proposed in the context of the NGST study (Next Generation Space Telescope) for high dynamic range imaging of exoplanets and other circumstellar materials (Boccaletti et al. 2000a; Moutou et al. 2000). Jupiter-like planets, 10^9 times fainter than their parent stars, may become detectable in the visible and near IR with a space-based coronagraph using refined cancellation techniques. Reaching the 10^9 contrast in ground-based telescopes is more challenging and current instruments are inadequate. Up to now, the search for faint companions by the mean of direct imaging was restrained to binary stars or low-mass stars. Beuzit et al. (1997) report a limiting sensitivity of $\Delta m_K = 12.4$ at $2''$ separation using the adaptive optics (AO) system

Send offprint requests to: A. Boccaletti

⋆ Based on observations collected at the European Southern Observatory, La Silla, Chile.

ADONIS and a Lyot coronagraph installed on the 3.6 m telescope at La Silla. The University of Hawaii AO system (Graves et al. 1998) features a detection threshold of $\Delta m = 14.7$ in the J band at $2''$ from the central star (Close et al. 1998). Actually, the typical angular separation of a Jupiter-like planet placed at 10 pc is only $0.5''$, and its detection requires a sensitivity of $\Delta m = 22$ in both visible and NIR spectral ranges (for 5 Gyr old). Nevertheless, according to the non-gray theory of Burrows et al. (1997), younger and/or heavier exo-planets may be significantly brighter ($m_K \sim 16$ for a $10^{6.5}$ yr-old and a 3 $M_{\rm jup}$ planet) and could become detectable with current instrumentation in the near IR as pointed out by Neuhäuser et al. (2000).

Since the dark-speckle method requires exposures shorter than the turbulence lifetime, photon-counting devices are best adapted to map the occurrence of zero photon-events on each frame. Photon-counting devices are not yet available in the infrared range, while most of the AO systems work in this part of the spectrum. However, NICMOS cameras are characterized by a significant read-out noise of a few tens of photo-electrons/pixel, and are expected to be less efficient regarding the dark-speckle method. Indeed, the dark speckles are no longer dark enough since owing to the readout noise a near IR detector is unable to record zero electrons. Nevertheless, we have expected that this technique could be implemented on a NICMOS detector if looking at very bright stars (see Sect. 4).

The ADONIS system has been selected to assess the feasibility of dark-speckle imaging in the near IR. We have obtained a total of 6 nights in period 62 (September 1998) and 63 (May 1999) to use the SHARP detector and the coronagraphic pre-focal optics. About 50% of telescope time was lost owing to malfunctions of the mechanical shutter.

The immediate objectives of our observing runs were:

- to test the dark-speckle method in the near IR by observing known binary stars;
- to search for unknown companions around bright stars, closer to the star ($\rho \lesssim 1''$) than could be done previously with classical coronagraphy.

In Sects. 2 and 3 we describe the instrument and the reduction process. The application of the dark-speckle data reduction to the near IR is described in Sect. 4. Section 5 presents the results, and Sect. 6 discusses the achievements.

2. Instrument description and observing strategy

2.1. The instrument

ADONIS is an adaptive optics system (Bonaccini et al. 1997) installed on the 3.6 m telescope at La Silla, and providing atmospheric seeing compensation in the near IR region (NIR hereafter). The SHARP II camera is a NICMOS 3 256×256 array detector equipped with standard broad band filters (J, H, K, SK) and several narrow band filters. Some technical features of SHARP are summarized in Table 1.

Table 1. Characteristics of SHARP II detector

Wavelength range	1−2.5 μm
Array size	256×256
Pixel size	40 μm
Pixel sampling	100, 50, 35 mas/pixel
Quantum efficiency	∼60%
Minimal exposure time	20 ms (shutter mode) 400 ms (electronic mode)
Read-out time	800 ms
Read-out noise	38 e^-/pixel ∼4 ADU/pixel

The stellar Lyot coronagraph available as pre-focal optics is fully described in Beuzit et al. (1997). Several mask can be selected, with diameters ranging from $0.43''$ to $6.17''$. The smallest masks ($0.63''$ and $0.84''$) have been used in this observing run to achieve very close angular separations and also because the dark-speckle method deals only with the speckle halo where faint companions are most probable (typically extending to $1.5''$). However, these masks are of poor efficiency to attenuate the starlight, the Lyot stop in the relayed pupil being optimized for larger Lyot masks (Mouillet 1997).

The SHARPII camera is not the ideal detector for implementing speckle techniques but it remains of interest to assess the feasibility of dark-speckle in the near IR. The high read-out noise and long read-out time affect the observing efficiency. The efficiency of the dark-speckle method depends on the wavelength range and on the short exposure duration. These parameters have to be accurately adjusted to provide speckle patterns with high contrast.

2.2. Wavelength range

To benefit from a maximum Strehl ratio, we observed at the longest wavelength available with the detector, in the 2.2 μm band, providing a $0.13''$ angular resolution. With a sampling of 35 mas/pixel, this corresponds to a linear speckle sampling of 3.7 pixels.

Although the speckle smearing arising from image chromaticity is a good criteria to pick out some real companions from the speckle field, this effect tends to fill in the area of destructive interferences in the focal plane, then reducing significantly the dark-speckle efficiency. To reduce the speckle smearing we used narrow band filters with spectral resolution larger than 50. This is the requirement to avoid a significant loss of contrast up to a radial distance of $10\lambda/D$. The CVF filter ($R \approx 60$) was mostly used, but the SK filter ($\lambda = 2.154$ μm, $\Delta\lambda = 0.323$ μm) was nevertheless necessary for faint stars (typically $m_K > 3.5$).

2.3. Integration time

Short exposures are used to freeze the speckle pattern and to allow dark-speckle processing (Labeyrie 1995). The integration time was scaled from visible observations using a $\lambda^{6/5}$ power law. Since the speckle lifetime in the visible (0.8 μm) is about 10 ms to 20 ms, we adopted an average value of 60 ms at 2.2 μm. Nevertheless, correlation times ranging from a few to hundreds of milliseconds have been observed, depending on the wind speed. However, these atmospheric conditions were not stable enough to modify the short exposure duration along the night.

In addition, the overheads are large due to the readout time of 800 ms.

3. Data reduction

3.1. Observing mode

The data acquisition and reduction process is adapted from Beuzit et al. (1997). The star is first observed without any coronagraphic mask to provide a relative photometric calibration. Then, short exposure data cubes are recorded with the coronagraphic mask occulting the bright central star (including the Airy peak and a few rings). In most cases, a data cube consists of 200 individual exposures, each lasting 60 ms. Sky frames are recorded in nodding mode by moving the telescope 30″ away from the star.

The sequence is repeated on a reference star. Indeed, despite the coronagraph, the wings of the PSF may remain brighter than faint companions or surrounding circumstellar material. In addition, the presence of an occulting mask in the focal plane prevents the application of classical deconvolution since the object-image relationship is no longer valid. The residual light can be partly subtracted with a reference star (with similar spectral type and magnitude) chosen angularly close to the star in order to get both 1/ similar seeing conditions and 2/ similar adaptive compensation. The star position accuracy using the chopping mirror is smaller than the pixel size on the detector (∼10 mas), but not sufficient for coronagraphy with small Lyot masks and without any systematic criteria. The most critical is to obtain similar positionning for the star and the reference relatively to the mask while the atmospheric seeing varies on a short timescale. Map subtraction is therefore never perfect especially when the PSF shape is changing.

3.2. Calibration of instrumental artifacts

Usual flat-fielding techniques were applied to the raw images. Once data cubes were corrected using these calibration data and the standard process, the frames could be co-added to provide a long exposure image or processed with a dark-speckle analysis.

4. Dark-speckle analysis

4.1. Implementation of the dark-speckle method in the near IR

The dark-speckle analysis is applied to the cleaned data cube for both the star and the reference. With a photon-counting device, the dark-speckle algorithm is straightforward since the occurrences of dark speckles are connected to the number of zero-photon events (Labeyrie 1995). With a detector featuring significant read-out noise (RON), the "bottom" of the dark speckles is no longer perfectly dark, even with short exposures and large spectral resolution. The efficiency of the dark-speckle technique is therefore decreased and the algorithm has to be modified. Assuming that the RON has Gaussian distribution, with a mean $\overline{k_\mathrm{b}}$ and a variance σ_b^2, the signal to noise ratio (SNR) is given by:

$$SNR_{\mathrm{RON}} = SNR_{\mathrm{ph-count}} \sqrt{\frac{\exp\left(-\frac{\overline{k_\mathrm{b}}^2}{2\sigma_\mathrm{b}^2}\right)}{\sqrt{2}\pi\sigma_\mathrm{b}}} \qquad (1)$$

where $SNR_{\mathrm{ph-count}}$ is the SNR obtained with a photon-couting camera as given in Boccaletti et al. (1998a). Equation (1) shows that the SNR is greatly affected when $\sigma_\mathrm{b} > 1$.

To implement the dark-speckle algorithm on a nIR detector, one has to define a threshold (ϵ) with respect to the RON. The detector areas with an intensity lower than this threshold are then assumed to be dark speckles. In the photon-couting mode, $\epsilon = 0$. In general, the threshold has to be optimized with respect to the companion intensity, as shown in the following sections. For very faint companions, the intensity of which is close to the read-out noise level, we initially assumed that $\epsilon \approx 3\sigma_\mathrm{b}$. But actually, the intensity of dark-speckles on short exposures is higher than σ_b and depends on the star's brightness. Moreover, the dark speckle level is not constant across the field but exhibits a radial dependence with respect to the central source. We checked that these artifacts do not originate from speckle smearing provided by the spectral range or the exposure time. This could be an internal effect due to scattering or remanence inside the detector itself, which cannot be corrected a posteriori.

The value $\epsilon(\rho)$ (where ρ is the radial distance to the star) is estimated on concentric rings with increasing radius centered on the occulted star. A numerical procedure derives the minimum averaged intensity on each ring and for each frame. The $\epsilon(\rho)$ profile has been found stable with time. Figure 1 shows an example of radial threshold used in the dark-speckle algorithm.

Once processed with the dark-speckle analysis for both the star and the reference, the data cubes are co-added to provide a "dark-speckle image" appearing in negative form since the dark speckles denotes a lack of light. Then, the reference star is subtracted after re-centering and proper scaling in intensity.

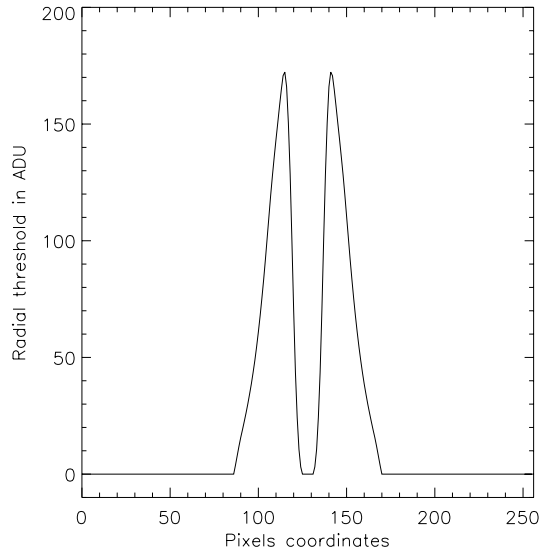

Fig. 1. An example of radial threshold obtained for the star HD 222493. A mask is used to select the region of interest: pixel 86 to 170

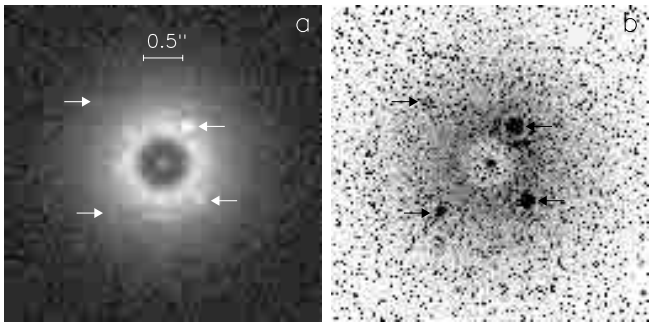

Fig. 2. Coronagraphic simulation of 200 frames each lasting 60 ms. Four companions (arrows) 5, 6, 7 and 8 magnitudes fainter than the star were added to the frames. The direct integration of frames is shown in **a)** and **b)** is the result obtained with a dark-speckle process on the same data cube (threshold: 10 ADU). Angular separation of the companions scaled to the resolution of a 3.6 m telescope at 2.2 μm are respectively 0.55″, 0.65″, 0.87″, 1.09″

4.2. Numerical simulation

Some numerical simulations have been carried out to assess the theoretical performance of the dark-speckle method using a near IR array with same characteristics as SHARP II. We therefore generated coronagraphic short exposures with realistic seeing conditions (providing a 45% Strehl ratio), photon noise and Gaussian read-out noise (38 e^-/pixel). Then we compared the direct integration of frames to the dark-speckle process. Figure 2 shows the simulation result for 200 frames of 60 ms. The star intensity is taken from real data ($\approx 3\,10^5$ ADU/frame equivalent to $m_K = 2$ star with a CVF filter and a 0.63″ mask). Faint companions with $\Delta m = 5$, 6, 7, 8, have been added to the frames. The speckle pattern is strictly assumed achromatic and frozen during the short exposures.

Only the 2 first companions ($\Delta m = 5$ and 6) are detected on the direct integration of frames (Fig. 2a). The other ones remain hidden in the halo of speckles. The dark-speckle process (Fig. 2b) is more efficient, and the gain in sensitivity is obvious since the third companion ($\Delta m = 7$) is clearly visible. The faintest companion ($\Delta m = 8$) is also marginally detected. As demonstrated with this simulation, the speckle noise originating from phase corrugation is markedly reduced through the dark-speckle analysis.

4.3. Signal to noise ratio measurement

As shown in the following sections, the detection of faint companions with a coronagraph is currently limited by the residual speckle pattern originating from both the atmospheric seeing and static aberrations. The calibration of these residual speckles is made critical by the temporal variation of seeing and flexures in the optical train, and then the reference star subtraction is not sufficient to remove the speckle noise. The derivation of the SNR using the global intensity deviation of the halo around the Lyot mask usually leads to optimistic values. Indeed, some speckles can be very bright relative to the average intensity of the halo but slightly contributes to the SNR calculation although they can be confused with a real companion. In this paper, we compare the intensity of the companion (integrated over 25 pixels $\equiv$ speckle area) with the averaged intensity of several bright residual speckles in the subtracted image to derive a more realistic SNR. Obviously, the selection of these residual speckles differs from a star to one another and sometimes from a direct integration to a dark-speckle image. But the principle of the process is strictly identical for the long exposure and the dark-speckle data.

The dark-speckle analysis is not more efficient than the direct imaging regarding the fixed speckle noise originating from static defects and pupil diffraction (waffle for instance). In both case frame subtraction of a reference is mandatory.

5. Results

Several bright single stars or binaries with known companions have been observed. Table 2 gives a list of all the stars observed in this program. In this section we present only the relevant results.

5.1. HD 222493

The binary star HD 222493 ($m_K = 3.80$, K0III) and the reference star HD 223170 ($m_K = 3.38$, K0III) have been observed twice, respectively in short exposure and long exposure modes. Frames lasting 60 ms were recorded with the SK filter ($\lambda = 2.154$ μm, $\Delta\lambda = 0.323$ μm) using a 0.63″ coronagraphic mask. Figure 3 shows the images obtained after co-adding 600 frames. The companion is evidenced on the direct image (Fig. 3a) but remains fainter than residuals partly originating from the spider arms

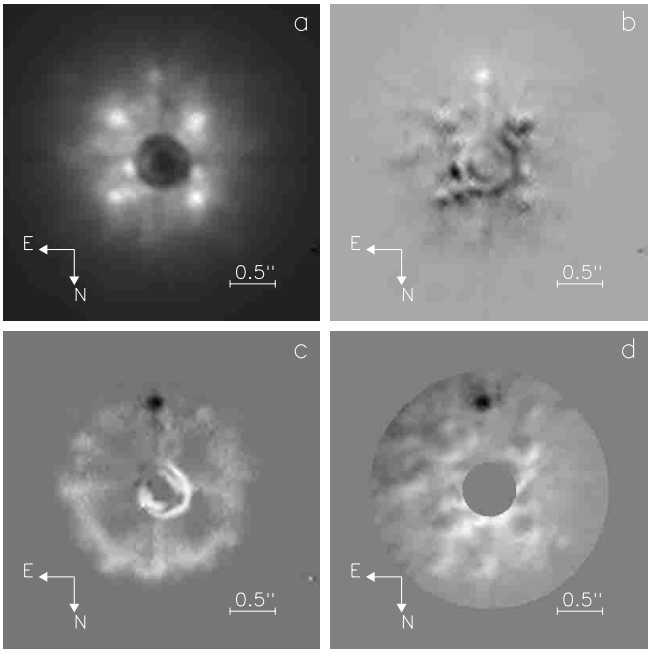

Fig. 3. Coronagraphic images of the binary star HD 222493 obtained with 600 frames lasting 60 ms each and a 0.63″ mask. The companion is already visible on the direct integration of frames **a)** and is enhanced on the subtraction map **b)**. Lower images **c,d)** show the subtraction result using dark-speckle process with a constant threshold of 100 ADU **c)** and a radial threshold **d)**, see Sect. 4. The companion now appears as a dark feature with an improved SNR

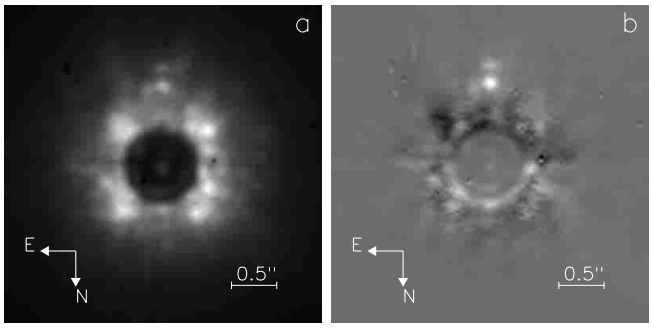

Fig. 4. Images of HD 222493 **a)** obtained under good seeing conditions and long exposures (18 × 2 s). The first companion's Airy ring is detectable on the subtraction frame **b)**

diffraction. Reference star subtraction (Fig. 3b) significantly improves the detectability ($SNR = 14.6$) but the contrast is clearly enhanced ($SNR = 26.7$) with a dark-speckle analysis (Figs. 3c,d). The companion is detected at $\rho = 0.89 \pm 0.04''$ away from HD 222493 with a position angle PA $= 178.3 \pm 0.2°$. The error bars come from the relative uncertainty between the star and the mask center coordinates. We compared the intensity of the companion and the star imaged off-axis, taking into account the halo contribution estimated at the same location on the reference star to derive from Fig. 3a the magnitude difference in the K band: $\Delta m_K = 3.8 \pm 0.2$. This reduction process is detailed in Boccaletti et al. (2000b).

These results are consistent with the Hipparcos data (ESA 1997): $\rho = 0.913''$, PA $= 183°$ and $\Delta m_V = 3.96$. The companion's spectral type can be coarsely determined from the $V_B - K_B = 2.25$ color index, leading to a K3V or G9III star, for which the typical masses are in agreement with the difference of 5° in position angle.

We later obtained long exposure images of HD 222493, co-adding 18 frames each lasting 2 s. The total integration time (36 s), as the number of detected photons, are the same as for the short exposure data. As shown in Fig. 4, the companion is easily detected with a $SNR = 23.5$, comparable to the one obtained using dark-speckle with short exposures. The first Airy ring of the companion featuring a typical triple aberration is noticeable. However, the variance of the halo intensity fluctuations is about 5 times larger in Fig. 3 than in Fig. 4. and the mask size has been increased from 0.63″ to 0.84″. If scaled to seeing condition closer to the previous one, the long exposure SNR would have been significantly lower. It is difficult in this case to compare the respective capability of short and long exposures. Nevertheless, one should notice that the SNR obtained in 36 s using direct integration mode is comparable with a dark-speckle process requiring about 516 s of telescope time (including readout time).

5.2. α Oph

The nearby star α Oph ($m_K = 1.65$, A5III) and its reference HD 161868 ($m_K = 3.78$, A0V) have been observed with the Circular Variable Filter (CVF, $\lambda = 2.15$ μm, $\Delta\lambda = 0.032$ μm) and a 0.63″ mask.

A companion is significantly detected on a 12 s integration (200 frames of 60 ms) at $\rho = 0.77 \pm 0.04''$ and PA $= 116.3 \pm 0.2°$. We measured a magnitude difference of $\Delta m_K = 3.5 \pm 0.2$. Figures 5a,b show the effect of the atmospheric variations on the direct integration. The SNR is 16.4 in Fig. 5a while it improves to 29.0 in Fig. 5b. However, the seeing was apparently stable: 1.07″ and 0.97″ respectively, but the speckle pattern has clearly evolved. This difference is explained by the time lag between the star and the reference: 23 min in Fig. 5a and 11 min in Fig. 5b. No significant improvement has been obtained once processed with a dark-speckle algorithm ($SNR = 12.1$ in Fig. 5c and 30.1 in Fig. 5d). Given the brightness of the companion ($m_K = 5.15$) we used a large radial threshold (∼1150 ADU at maximum) to avoid saturation of the dark-speckle frames. Actually, the threshold has to be optimized with respect to the intensity of the companion. As a drawback, the dynamic range is largely reduced and for instance the companion Airy ring's is no longer visible in Fig. 5d with opposite to Fig. 5b. Nevertheless, a lower threshold would optimize the detection of this secondary pattern.

Comparison with the Hipparcos values is not straightforward since the period is short ($P = 8.7$ years) and the eccentricity is large ($e = 0.804 \pm 0.045$, Kamper et al. 1989). Despite the poor accuracy obtained with Hipparcos for this star, the solution is in agreement with our

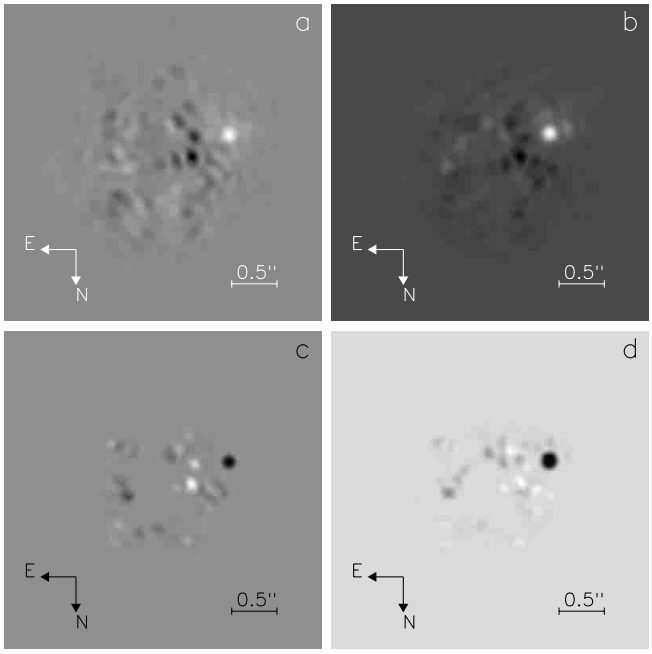

Fig. 5. Subtracted maps of the star α Oph with direct integration of frames in two different atmospheric conditions **a,b)** and processed with a dark-speckle analysis **c,d)**

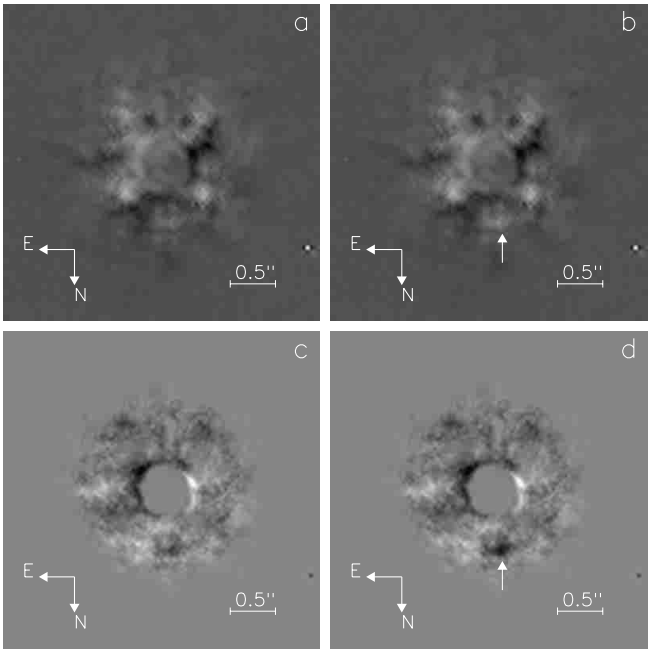

Fig. 6. Coronagraphic subtracted images of HD 192876 for direct integration of frames **a,b)** and with a dark-speckle analysis **c,d)**. A faint companion ($\Delta m_k = 6$, arrow) is added to the map **b,d)** to assess the detection threshold. The SNR is 1.8 with a direct integration and improves to 4.8 owing to the dark-speckle process

result: $0.5'' < \rho < 0.7''$ (Martin & Mignard 1998). The position angle is not indicated. The magnitude difference in the V band derived by Martin & Mignard (1998) is: $\Delta m_V = 5.23$. An older estimate of the brightness ratio is given by Kamper et al. (1989) in the L band (3.4 μm) using IR speckle interferometry: $\Delta m_L = 3.5$, which is identical to the K band result. Given the color indexes $V_B - K_B = 2.18$ and $V_B - L_B = 2.22$ together with the individual masses (4 $M_\odot$ and 0.7 $M_\odot$) infered from astrometry (Martin & Mignard 1998), we assumed a K2V spectral type for the secondary star. The absolute magnitude $M_v = 6.55$, derived from the parallax (69.84 mas) is also in accordance with a K2V companion.

5.3. HD 192876

The binary star HD 192876 ($m_K = 1.92$, G3Ib) and the reference star HD 192947 ($m_K = 1.41$, G8III) were observed in both short and long exposures using the CVF ($\lambda = 2.06$ μm, $\Delta\lambda = 0.031$ μm) and a $0.63''$ mask. Unlike the result announced by Hipparcos in the visible ($\rho = 0.65''$, PA $= 355°$, $\Delta m_V = 4.17$), the companion was not detectable in the nIR spectrum, even with an integration of 1200 s. Nevertheless, these data were of interest to assess the lower limit of the faint companion's magnitude difference in the K band, and also to evaluate the present sensitivity of the dark-speckle analysis.

Using a set of 400 frames lasting 60 ms, an attenuated copy of the star observed off-axis was added to each frames at the location expected by Hipparcos. Then, the brightness of this artifical companion was decreased down to the detection threshold. Figure 6 shows the subtracted images with the companion turned on and off for both the direct integration of frames and the dark-speckle analysis. The added companion is 6 magnitudes fainter than the star and is significantly detected ($SNR = 4.8$) owing to the dark-speckle process (Fig. 6d, arrow), but remains invisible in Fig. 6b (arrow). We therefore estimate the sensitivity of direct integration to $\Delta m_K \approx 6$ in the present case and to $\Delta m_K \approx 7.5$ using dark speckles. One has to notice that the efficiency of the dark-speckle process is emphasized here unlike the case of HD 222493. Actually, the present case is less affected by speckle smearing since the bandwidth is smaller ($\Delta\lambda = 0.031$ μm) than the one used for HD 222493 ($\Delta\lambda = 0.323$ μm). Also, this example shows that the dark-speckle analysis is more appropriate to large magnitude differences, as predicted in Boccaletti et al. (1998a).

5.4. η Psc

Owing to the shutter malfunction, 50% of the telescope time was devoted to direct imaging of faint companions using long exposures. It was precisely the case for the star η Psc ($m_K = 1.43$, G7IIa) and its reference HD 10761 ($m_K = 2.14$, G8III). 100 coronagraphic images, each lasting 4 s, were recorded with a $0.84''$ mask and a CVF filter ($\lambda = 2.06$ μm, $\Delta\lambda = 0.031$ μm).

The hypothetic companion appears on the subtracted image (Fig. 7b) at position: $\rho = 0.54 \pm 0.04''$ and PA $= 74.2 \pm 0.2°$ with $SNR = 3.2$. When compared to the star flux, we derive a $\Delta m_K = 3.7 \pm 0.2$. However, this result

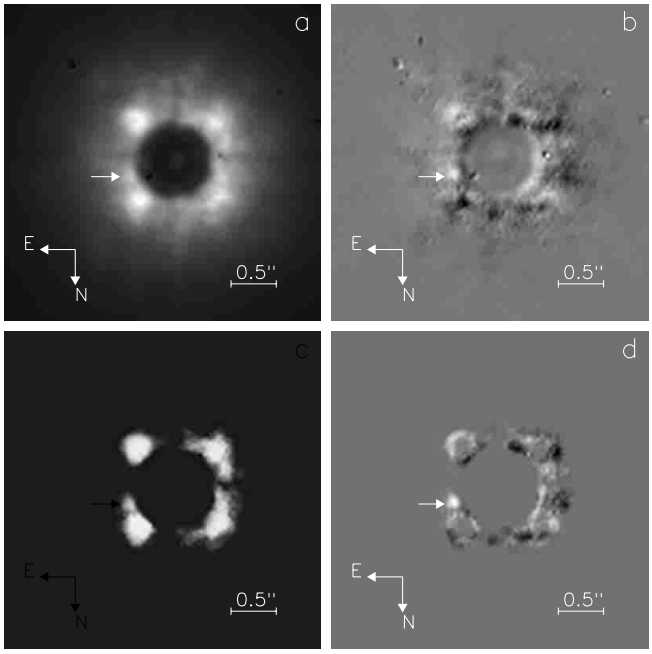

Fig. 7. Coronagraphic images of η Psc **a)** and the result of reference star subtraction **b)**. Lower images show the dark-speckle process for the star alone **c)** and the subtraction **d)**. The suspected companion is indicated by an arrow

is not consistent with the Hipparcos value: $\rho = 0.64''$, PA $= 47°$ and $\Delta m_V = 3.7$, as already mentionned in Boccaletti et al. (1998b). The discrepancy mainly turns on the position angle, with a significant difference of 27.2°. To explain such a large difference, the companion has to be a massive star, like the primary one.

Although the exposure time of each frame (4 s) was longer than the turbulence life-time, the data cube of η Psc was processed with dark-speckle analysis. Obviously, the threshold is very high: 9000 ADU for η Psc and 4900 ADU for HD 10761, since the speckle pattern is smeared on 4 s frame and the photon flux per frame is larger. The results are presented in Fig. 7. The subtraction frame (Fig. 7d) evidenced the "dark pattern" (arrow) with a $SNR = 4.2$, a slight improvement of about 30% compared to the direct integration of frames ($SNR = 3.2$, Fig. 7b). This suspicious detection would required to be confirmed by further observations.

5.5. υ Oph

υ Oph ($m_K = 4.38$, A3 m) is a binary star listed in the Hipparcos catalogue with a relatively large magnitude difference in the visible ($\Delta m_V = 4.12$). Actually, the companion is easily detectable with ADONIS in the near IR since the magnitude difference is $\Delta m_K = 2.36$ (see Fig. 8). The dark-speckle analysis is therefore not required in this case. From short exposures data cube recorded at 2.12 μm (CVF), we derive the location of the companion: $\rho = 0.48 \pm 0.04''$ and PA $= 315 \pm 0.2°$ in disagreement with the Hipparcos measurement: $\rho = 0.458''$ and PA $= 209°$. Here, the companion is fairly bright in our

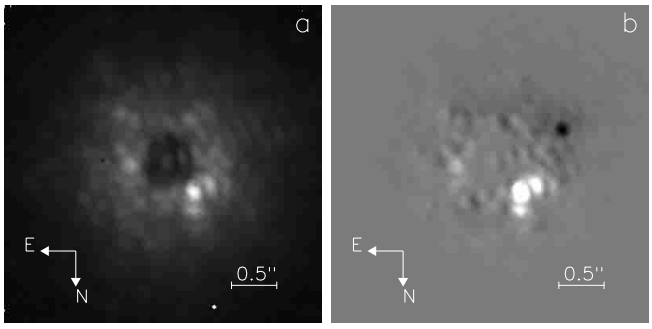

Fig. 8. Coronagraphic images of υ Oph, displayed with a 0.5 power **a)**. The subtraction with α Oph is also shown **b)**. The companion of α Oph is visible as a dark feature

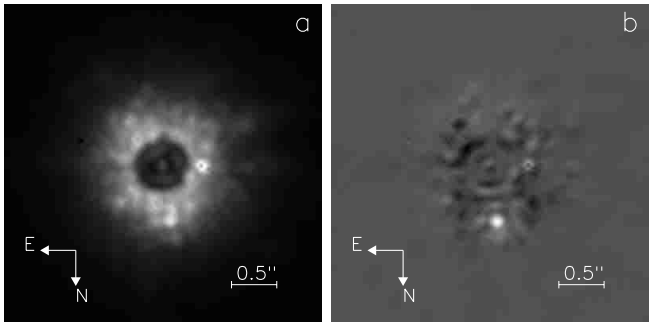

Fig. 9. Coronagraphic image of HD 184713 using long exposures **a)** and the subtraction map **b)** where the companion is clearly evidenced with its first bright Airy ring

image (Fig. 8) and its direct detection cannot be questionned ($SNR = 61.8$). The $V_B - K_B = 2.00$ color index, together with the absolute magnitude $M_v = 5.89$ (parallaxe of 26.67 mas) suggest a K1V spectral type. Assuming a typical mass of 0.79 $M_\odot$ and a semi-major axis of at least $0.48''$, a pole-on orbit would have a period of 42 years, leading to a significant angular movement of about 64°, but however too small compared to the difference of 106° between the Hipparcos measurement and our result. This object could also be a background star, but in this case the true companion should have been detected as another feature of same brightness (at PA $= 273°$ if the orbit is pole-on).

5.6. HD 184713

The last binary star presented in this paper is HD 184713 ($m_K = 6.20$, K0III) and its reference HD 184869 ($m_K = 7.06$, G8III). Given the faintness of these objects, we used the broad band SK filter, and long exposures of 10 s each. The relatively stable atmospheric seeing ($0.70''$ on average) allowed us to combine 60 frames totalling 600 s of integration, for both the star and the reference. Unlike the images presented hereabove and despite the long integration time, the residual speckle pattern in Fig. 9a is still visible denoting a low and stable seeing ($\sim 0.7''$). Then, owing to stable conditions, the subtraction process in Fig. 9b is very efficient to extract faint objects

Table 2. List of stars in our program with the derived parameters (Δm_K, ρ, θ) compared to other references. $^{(H)}$ indicates the Hipparcos values

Stars	m_K	Δm_K	ρ,θ	Other ref.
HD 194943	3.84	1.30	1.23″, 195°	1.21″, 193° $^{(H)}$ $\Delta m_V = 2.05$
HD 192876	1.92	-	-	0.65″, 355° $^{(H)}$ $\Delta m_V = 4.17$
HD 222493	3.54	3.80	0.89″, 178°	0.913″, 183° $^{(H)}$ $\Delta m_V = 3.96$
o Cet		-	-	0.578″, 108°
η Psc	1.43	3.70	0.54″, 74°	0.64″, 47° $^{(H)}$ $\Delta m_V = 3.7$
AB Dor		-	-	$0.2'' \sim 0.7''$ $\Delta m_K = 3 \sim 4$
HD 91416	3.72	-	-	0.486″, 210° $^{(H)}$ $\Delta m_V = 3.90$
GL 538.1	0.72	-	-	-
GL 539	−0.20	-	-	-
β Sco	2.77	2.7	0.6″, 180°	0.5″
τ Sgr	0.63	-	-	-
HD 71129	−1.06	-	-	0.46″ $\Delta m_K = 6.2$
GL 570A	3.15	-	-	-
υ Oph	4.38	2.36	0.48″, 315°	0.458″, 209° $^{(H)}$ $\Delta m_V = 4.12$
α Oph	1.65	3.77	0.77″, 116°	$0.2'' \sim 0.7''$ $\Delta m_V = 5.23$
29 Sgr	1.83	-	-	-
GL 664	3.58	-	-	-
HD 184713	6.56	4.93	0.63″, 351°	0.632″, 350° $^{(H)}$ $\Delta m_V = 3.29$
GL 716	4.31	-	-	-

in the halo of speckles. The companion is unambiguously detected with a $SNR = 28.2$ at position $\rho = 0.63 \pm 0.04''$ and PA $= 351.2 \pm 0.2°$. This is the largest brightness ratio observed in our program with a $\Delta m_K = 4.9 \pm 0.2$, and we derive a detection threshold of 6.3 magnitudes difference for similar angular separation. This result is in very good agreement with the Hipparcos values: $\rho = 0.632''$ and PA $= 350°$. According to the color index ($V_B - K_B = 1.11$) and to the absolute magnitude ($M_v = 3.81$ for a parallaxe of 2.06 mas), the companion could be a F7V star.

6. Performance

6.1. Global coronagraphic performances with ADONIS

Faint companions with large magnitude differences lying in the close vicinity of the Airy pattern ($0.3'' < \rho < 1'' \Leftrightarrow 2.3\lambda/D < \rho < 7.7\lambda/D$) have been imaged. The achievable brightness ratio is limited by the residual speckle noise on short as well as on long exposures. This intrinsic limitation originates from a combination of the atmospheric conditions and the performance of the AO system. Most of the time, the coronagraph causes the appearance of static speckles close to the occulting mask which can be confused with faint companions (see for instance Figs. 8 and 9). Careful map subtraction is then required to clean-up the image from such artifacts and to improve the dynamic range.

In addition, the coronagraph used with the smallest masks (⌀: 0.63″, 0.84″) has very little effect on the detectability. It simply avoids the detector saturation. To improve the capability with small masks, the Lyot stop must be shrunk with respect to the pupil size. But the sensitivity of the instrument would be greatly affected.

The detection threshold allowed by the present instrument using short exposures is about $\Delta m_K = 6 \sim 7$ (depending on the primary star flux), 0.6″ away from the star. In principle, longer sequences would enhance the result, but then the stability of the Point Spread Function becomes problematic.

6.2. Performance of the dark-speckle analysis

Testing the feasibility of dark-speckle with ADONIS on the 3.6 m telescope was the prime goal of these observing runs. The stars listed in Sect. 5 allowed us to infer the performance of dark-speckle coronagraphy in the nIR. As a first result, we established the applicability of the method with nIR detector even with a significant RON, the algorithm being modified as described in Sect. 4. Nevertheless, with current detectors, the use of short exposures severely restricts the observation to the brightest stars.

To derive the sensitivity with short exposures, we assumed that the dark-speckle analysis can be applied if speckles ($>3\sigma$) are significantly detected. Thus, we compared the average flux of a speckle sampled on 16 pixels with the RON (38 e^-/pixel $\Leftrightarrow$ 152 e^-/speckle area). The speckle flux depending on the short exposure time ($t = 60$ ms), the spectral bandwidth ($\Delta\lambda$) and the radial distance (1.2″ corresponding to the halo extension) has to be at least 3 times higher than the total RON. Using the collected data, we measured a sensitivity of $m_K = 3.85$ for 60 ms exposures and using the CVF.

The efficiency of dark-speckle using short exposures is illustrated in Sects. 5.1, 5.2 and 5.3. The achievable SNR is markedly enhanced compared to direct integration of frames, and the gain is about a factor of 2 for bright companions and about 1.5 magnitudes at the detection threshold. Although the gain is significant, we did not detect any real faint companions exclusively with a dark-speckle process. However, the fake companion added to the image of HD 192876 is only detectable once the dark-speckle analysis is performed on the short exposures. This example points out the major interest of the dark-speckle method when the companion is fainter than residual speckles. Actually, to be more competitive, the

short exposure data cubes should contain a larger number of frames in order to increase the signal with respect to the read-out noise. The threshold of detection ($\Delta m = 6 \sim 7$) is in agreement with the result of numerical simulation (Sect. 4.2) although obtained without frame subtraction of the reference star. Indeed, the simulated wavefront has no temporal coherence and no static defects. As a consequence, the generated speckle pattern is strictly uniform, a more favorable case than for ground-based observations.

The lost time due to the shutter malfunction was finally avoided by using long exposures (see Sects. 5.4 and 5.6). As shown in the case of η Psc, and despite the duration of frames, the thresholding process is of interest to slightly improve the contrast of faint companions. Such an efficiency was somewhat unexpected before.

The selection of appropriate threshold on short exposures as well as on long exposures enables to achieve a better cancellation of the residual speckle pattern. This property is clearly demonstrated on map subtractions processed with dark-speckle.

In addition to the read-out noise, another drawback of using short exposures with ADONIS resides in the read-out time lasting about 800 ms. The observing time required for integrating hundreds of short exposures shorter than the read-out time is therefore considerably larger than in the long exposure mode. For instance, the detection of the companion of HD 222493 (Sect. 5.1) is achieved with a larger SNR using dark-speckle than with direct integration but for a telescope time 14 times larger. A fast read-out camera would be therefore favorable to the dark-speckle analysis. With identical telescope time, direct integration yields deeper images, but with identical integration time, short exposures may be of interest to detect companions fainter than speckle residuals around very bright stars.

6.3. Comparison with Hipparcos data

Some results obtained here are sometimes inconsistent with the Hipparcos data, mainly in terms of position angle. It is the case for 2 stars in our sample: η Psc and υ Oph. Although the detection of the η Psc companion could be questionned, it is not the case for υ Oph. The companion is indeed very bright and unambiguously detected. It is therefore suspected that for faint companions ($\Delta m_V \gtrsim 4$), the Hipparcos data could be of lower accuracy. In such a case a direct method (AO imaging + coronagraphy, for instance) is obviously more suited.

On the other hand, several companions found by Hipparcos are still invisible on nIR images (HD 192876 for instance). It suggests that the secondary stars would be of an earlier spectral type than the primary. Imaging in the visible will then be required to check this assumption.

Finally, some nearby single stars, selected from the Gliese catalogue, were included in our sample with the intent to search for unknown companions. Nevertheless, we did not infer the presence of any low-mass stars around these objects.

7. Conclusion

The implementation of the dark-speckle method in the nIR has been tested successfully on ADONIS, and its imaging capability of faint companions has been demonstrated. Although its application is restricted to stars brighter than $m_K = 4$ with the available detector, contrast of faint companions can be improved in a sub-arcsecond field.

The observations presented in this paper, have been useful to:

- calibrate the method in the nIR regarding the choice of filters, pixel sampling, number and duration of frames;
- assess the performance of the dark-speckle method in terms of achievable brightness ratio and angular separation;
- assess the effect of a significant RON on the detectability and sensitivity;
- prepare the implementation of such techniques on future instruments like the NAOS adaptive optics on the VLT or in space with the NGST.

Telescope time is obviously a major issue and the use of short exposures is less efficient than direct integration with NIR detector featuring a large readout time. The detector noise is also a major limitation since the sensitivity of short exposures is very low and restrained the observation to bright stars. But these former effects are less critical than the atmospheric seeing residue, for searching faint objects within the speckle halo. In this case, the dark-speckle method is of major interest especially for companions fainter than residual speckles and even using NIR system like ADONIS and SHARP II.

Finally, high contrast imaging with AO+coronagraph whether using long or short exposures is proved suitable to derive an accurate brightness ratio measurement and also a coarse estimate of the spectral type when coupled with other wavelength data.

Acknowledgements. We wish to thank the ESO-3.6 m team and especially F. Marchis for his efficient support during the allocated nights. We are also grateful to Antoine Labeyrie for helpful discussions and careful reading of the manuscript and to the referee for its constructive comments.

References

Abe, L., Vakili, F., & Boccaletti, A. 2000, A&A, submitted
Beuzit, J. L., Mouillet, D., Lagrange, A. M., & Paufique, J. 1997, A&AS, 125, 175
Boccaletti, A., Ragazzoni, R., & Labeyrie, A. 1998, A&A, 338, 106

Boccaletti, A., Moutou, C., Labeyrie, A., Kohler, D., & Vakili, F. 1998, A&AS, 133, 395
Boccaletti, A., Moutou, C., Abe, L., et al. 2000, Proc. of NGST Science and Technology exposition, ASP Conf. Ser., 207, 179
Boccaletti, A., Moutou, C., & Abe, L. 2000, A&AS, 141, 157
Bonaccini, D., Prieto, E., Corporon, P., et al. 1997, in Proc. Adaptive Optics and Applications, SPIE , ed. S. Diego
Burrows, A., Marley, M., Hubbard, W., et al. 1997, ApJ, 491, 856
Close, L. M., Dutrey, A., & Roddier, F. 1998, ApJ, 499, 883
ESA 1997, SP-1200
Gay, J., & Rabbia, Y. 1996, CR. Acad. Sci. Paris, t. 332, Serie II b, 265
Graves, J. E., Northcott, M. J., Roddier, F., et al. 1998, Proc. SPIE 3353, 34
Kamper, K. W., Legget, D., & McCarthy, D. W. 1989, AJ, 98, 686
Labeyrie, A. 1995, A&A, 298, 544
Martin, C., & Mignard, F. 1998, A&A, 330, 585
Mouillet, D. 1997, Ph.D. Thesis, Grenoble, France
Moutou, C., Boccaletti, A., Labeyrie, A., et al. 2000, Proc. of NGST Science and Technology Exposition, ASP Conf. Ser., 207, 484
Neuhäuser, R., Brandner, W., Eckart, A., et al. 2000, A&A, 354, L9
Roddier, F., & Roddier, C. 1997, PASP, 109, 815
Rouan, D., Riaud, P., Boccaletti, A., et al. 2000, PASP, 112, 1479
Trauger, J., Beichman, C., Djorgovski, et al. 1998, BAAS, 30, 1297